

THE LANCET

Infectious Diseases

Supplementary appendix

This appendix formed part of the original submission. We post it as supplied by the authors.

Supplement to: Wang Q, Li Z, Ho J, et al. Resistance of SARS-CoV-2 omicron subvariant BA.4.6 to antibody neutralisation. *Lancet Infect Dis* 2022; published online Oct 31. [https://doi.org/10.1016/S1473-3099\(22\)00694-6](https://doi.org/10.1016/S1473-3099(22)00694-6).

Supplementary Appendix

Table S1. Demographics of clinical cohorts in this study.

Sample ID	Vaccine type and infected strain	Days post-vaccination or *infection (after last exposure)	Documented COVID-19	Age	Gender
Boosted					
Q1	mRNA-1273/mRNA-1273/mRNA-1273	29	No	66	Female
Q2	BNT162b2/BNT162b2/BNT162b2	30	No	68	Male
Q3	BNT162b2/BNT162b2/BNT162b2	14	No	64	Female
Q4	BNT162b2/BNT162b2/BNT162b2	34	No	55	Male
Q5	BNT162b2/BNT162b2/BNT162b2	34	No	45	Male
Q6	BNT162b2/BNT162b2/BNT162b2	15	No	50	Female
Q7	BNT162b2/BNT162b2/BNT162b2	15	No	48	Female
Q8	BNT162b2/BNT162b2/BNT162b2	29	No	71	Male
Q9	BNT162b2/BNT162b2/BNT162b2	90	No	59	Male
Q10	BNT162b2/BNT162b2/BNT162b2	33	No	45	Male
Q11	BNT162b2/BNT162b2/BNT162b2	87	No	66	Female
Q12	BNT162b2/BNT162b2/BNT162b2	84	No	26	Male
Q13	mRNA-1273/mRNA-1273/mRNA-1273	23	No	28	Female
Q15	BNT162b2/BNT162b2/mRNA-1273	32	No	39	Male
BA.1 breakthrough					
Q24	BNT162b2/BNT162b2/BA.1	*14	Yes	Unknown	Unknown
Q25	BNT162b2/BNT162b2/BA.1	*14	Yes	Unknown	Unknown
Q26	mRNA-1273/mRNA-1273/BA.1	*35	Yes	Unknown	Unknown
Q27	BNT162b2/BNT162b2/BNT162b2/BA.1	*135	Yes	78	Male
Q28	BNT162b2/BNT162b2/BNT162b2/BA.1	*14	Yes	Unknown	Unknown
Q29	BNT162b2/BNT162b2/BNT162b2/BA.1	*14	Yes	Unknown	Unknown
Q30	BNT162b2/BNT162b2/BNT162b2/BA.1	*14	Yes	Unknown	Unknown
Q31	BNT162b2/BNT162b2/BNT162b2/BA.1	*41	Yes	48	Male
Q32	BNT162b2/BNT162b2/BNT162b2/BA.1	*26	Yes	38	Female
Q33	BNT162b2/BNT162b2/B.1.617.2/BNT162b2/BA.1	*19	Yes	35	Female
Q34	BNT162b2/BNT162b2/mRNA-1273/mRNA-1273/BA.1	*67	Yes	40	Male
Q41	WA1/BNT162b2/BA.1	*21	Yes	52	Male
Q42	WA1/BNT162b2/BA.1	*44	Yes	37	Intersex
BA.2 breakthrough					
Q35	BNT162b2/BNT162b2/BA.2	*14	Yes	50	Female
Q36	BNT162b2/BNT162b2/BNT162b2/Ad26.COVS.S/BA.2	*22	Yes	69	Male
Q50	mRNA-1273/mRNA-1273/mRNA-1273/BA.2	*14	Yes	34	Male
Q51	BNT162b2/BNT162b2/mRNA-1273/BA.2	*19	Yes	33	Female
Q52	BNT162b2/BNT162b2/mRNA-1273/BA.2	*18	Yes	29	Female
Q53	BNT162b2/BNT162b2/BNT162b2/BA.2	*25	Yes	34	Male
Q54	BNT162b2/BNT162b2/BNT162b2/BA.2	*36	Yes	37	Female
Q55	BNT162b2/BNT162b2/mRNA-1273/BA.2	*18	Yes	41	Female
Q56	mRNA-1273/mRNA-1273/mRNA-1273/BA.2	*21	Yes	36	Female
Q57	BNT162b2/BNT162b2/mRNA-1273/BA.2	*32	Yes	28	Male
Q58	BNT162b2/BNT162b2/mRNA-1273/BA.2	*23	Yes	33	Female
BA.4/5 breakthrough					
Q71	mRNA-1273/mRNA-1273/BNT162b2/BA.5.2.1	*29	Yes	29	Female
Q77	BNT162b2/BNT162b2/BNT162b2/BA.5	*22	Yes	61	Female
Q79	mRNA-1273/mRNA-1273/mRNA-1273/BA.5	*15	Yes	28	Female
Q80	mRNA-1273/mRNA-1273/mRNA-1273/BA.5	*21	Yes	24	Female
Q81	BNT162b2/BNT162b2/BNT162b2/BA.5	*75	Yes	35	Female
Q82	BNT162b2/BNT162b2/mRNA-1273/BA.5	*63	Yes	46	Female
Q83	BNT162b2/BNT162b2/BNT162b2/BA.5	*28	Yes	55	Male
Q84	BNT162b2/BNT162b2/BNT162b2/BA.5	*17	Yes	57	Female

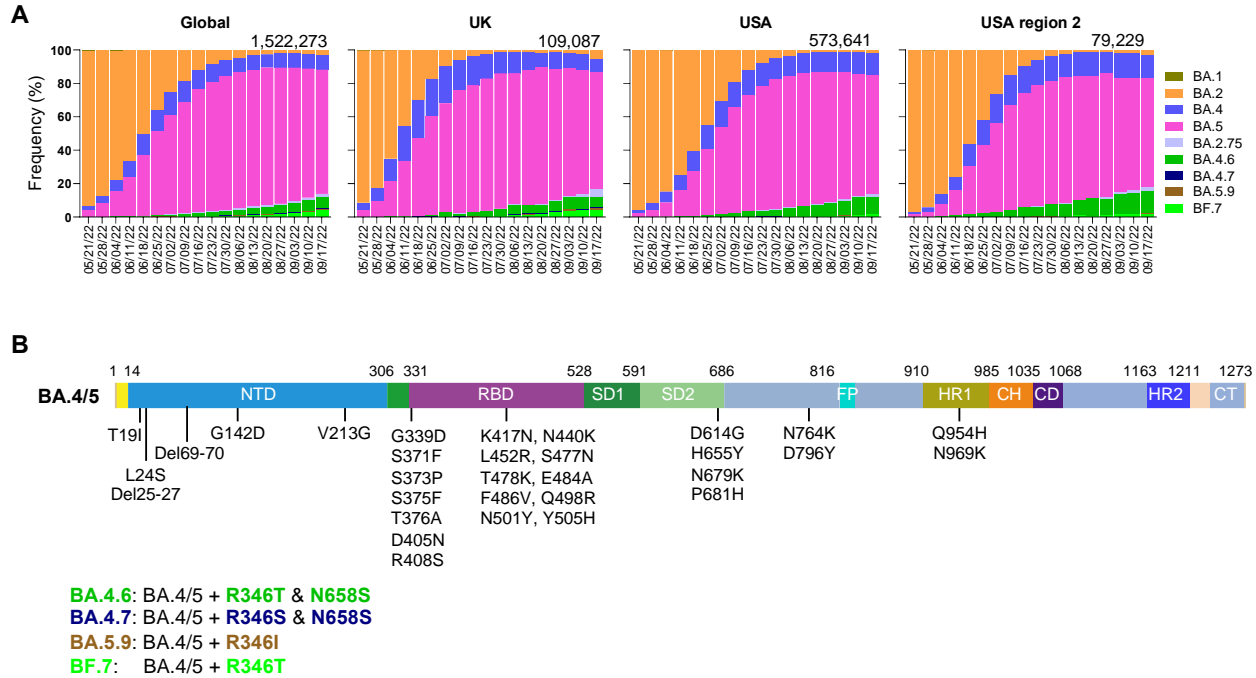


Figure S1. Prevalence of Omicron subvariants and mutations found in BA.4.6 spike.

- A. Frequencies of Omicron subvariants deposited in GISAID. The value in the upper right corner of each box shows the cumulative number of sequences for all circulating viruses in the denoted time period. USA region 2 includes New Jersey, New York, Puerto Rico, and Virgin Islands.
- B. Spike mutations found in BA.4.6 relative to BA.4/5. NTD, N-terminal domain; RBD, receptor-binding domain; SD1 and SD2, subdomains 1 and 2. FP, fusion peptide; HR1 and HR2, heptad repeat region 1 and 2; CH, central helical region; CD, connector domain; TM, transmembrane region; CT, cytoplasmic tail. The amino acid changes in the BA.4/5 spike relative to the D614G are shown in the diagrams.

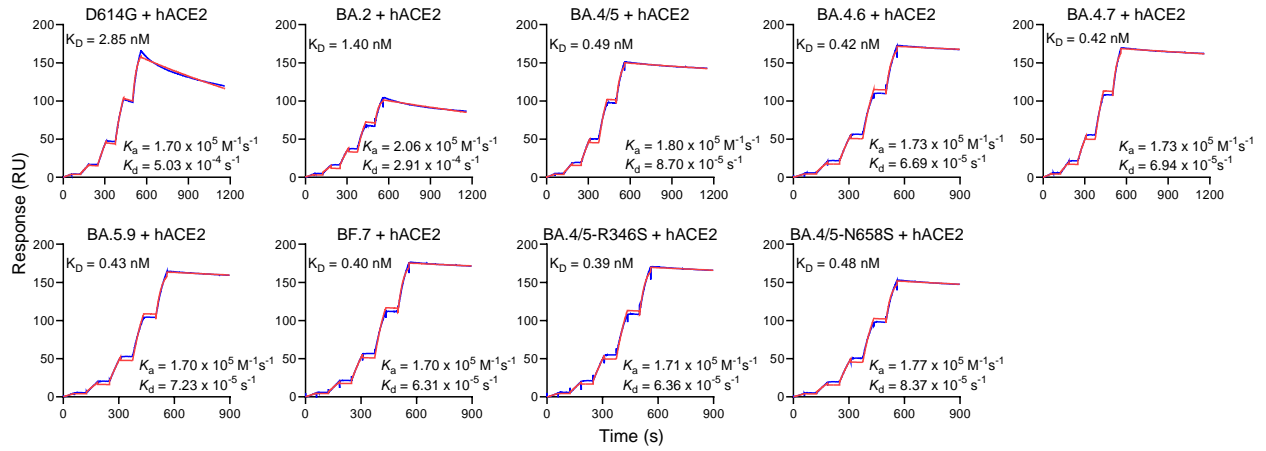


Figure S2. Binding affinities of Omicron subvariant spike trimer proteins to hACE2 as measured by SPR.

IC ₅₀ (µg/mL)	non-RBD mAbs			RBD mAbs																		Combination						
	NTD	NTD-SD2	SD1	Class 1						Class 2			Class 3						Class 4									
	C1520	C1717	S3H3	Brii-196	CAB-A17	Omi-3	Omi-18	BD-519	COVOX-222	XGv347	ZCB11	COV2-2196	XGv282	LY-CoV1404	S309	XGv289	Brii-198	2-7	COV2-2130	BD55-5840	BD55-3152	BD-804	10-40	COV2-2130 + COV2-2196	Brii-196 + Brii-198			
D614G	0.0038	0.350	0.044	0.024	0.014	0.008	0.025	0.022	0.020	0.002	0.005	0.003	0.0003	0.0615	0.066	0.0009	0.436	0.008	0.008	0.002	0.004	0.021	0.090	0.003	0.034			
BA.2	0.0013	0.503	0.012	1.576	0.025	0.012	0.004	0.009	0.171	0.003	0.007	0.958	0.0003	0.0011	1.320	0.055	2.597	0.036	0.014	0.012	0.045	0.046	5.274	0.029	3.992			
BA.4/5	0.0016	0.271	0.017	0.730	0.014	0.023	0.009	0.009	0.063	1.174	1.489	>10	0.0010	0.0012	2.534	0.060	>10	0.067	0.061	0.014	0.064	0.027	6.812	0.074	2.177			
BA.4.6	0.0013	0.216	0.016	0.909	0.016	0.026	0.011	0.009	0.039	0.903	1.725	>10	0.0005	0.0012	2.679	0.141	>10	0.060	>10	2.048	>10	>10	7.038	>10	2.119			
BA.4.7	0.0012	0.204	0.015	0.531	0.018	0.039	0.012	0.009	0.049	1.899	1.647	>10	0.0006	0.0010	1.440	0.061	>10	0.041	>10	0.942	>10	>10	3.189	>10	1.195			
BA.5.9	0.0007	0.315	0.019	0.466	0.018	0.035	0.016	0.010	0.041	0.858	1.253	>10	0.0005	0.0009	3.188	0.089	>10	0.057	>10	3.006	>10	>10	4.458	>10	1.000			
BF.7	0.0023	0.290	0.021	0.604	0.017	0.034	0.016	0.010	0.060	0.684	0.972	>10	0.0011	0.0016	3.218	0.041	>10	0.051	>10	0.840	>10	>10	6.261	>10	1.061			
BA.4/5-R346S	0.0007	0.333	0.025	0.754	0.024	0.040	0.014	0.010	0.046	0.753	1.132	>10	0.0005	0.0007	4.939	0.069	>10	0.046	>10	0.959	>10	>10	6.562	>10	1.533			
BA.4/5-N658S	0.0005	0.185	0.019	0.345	0.020	0.026	0.012	0.007	0.032	0.688	1.668	>10	0.0005	0.0006	1.414	0.079	>10	0.076	0.055	0.010	0.046	0.083	6.447	0.092	1.168			
																							>10	1-10	0.1-1	0.01-0.1	0.001-0.01	<0.001

Figure S3. Neutralization IC₅₀ titers for indicated pseudoviruses by mAbs.

The brand names of therapeutic neutralizing antibodies in the table are: Brii-196 (amubarvimab), COV2-2196 (tixagevimab), LY-CoV1404 (bebtelovimab), S309 (sotrovimab), Brii-198 (romlusevimab), COV2-2130 (cilgavimab). Antibody combinations: Evusheld consists of tixagevimab co-packaged with cilgavimab, and the Brii cocktail combination consists of amubarvimab and romlusevimab. Background colors indicate neutralization levels.

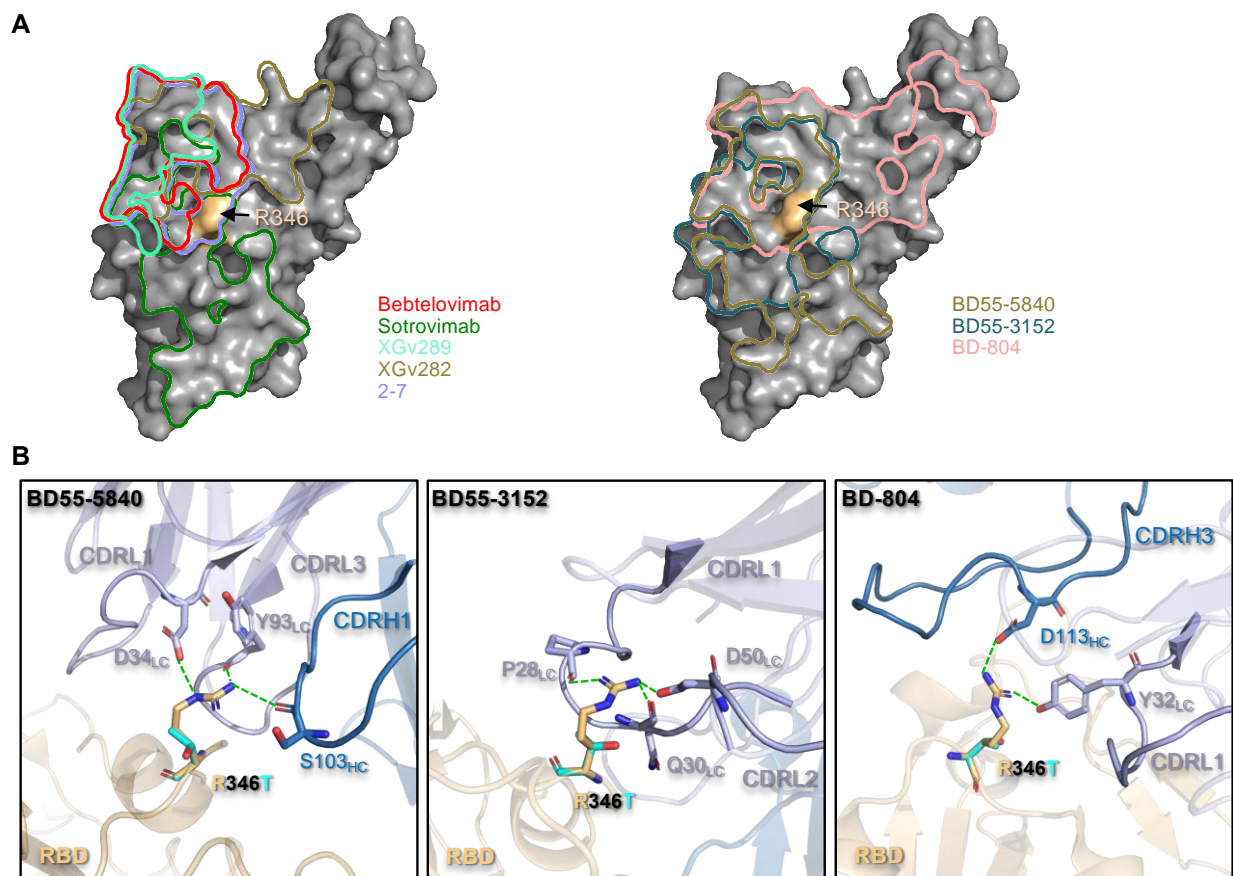


Figure S4. Modeling of how R346T affects RBD class 3 mAb neutralization.

A. Footprints of class 3 neutralizing mAbs on the RBD.

B. Structural analysis for how R346T affects RBD class 3 mAbs binding. The green dashed lines denote the hydrogen bond and the salt bridge.

The structures of antibody-spike complexes were obtained from Protein Data Bank (7MMO for bebtelovimab, 6WPS for sotrovimab, 7WEF for XGv289, 7WLC for XGv282, 7LSS for 2-7, 7X6A for BD55-5840, 7WR8 for BD55-3152, and 7EYA for BD-804) for modeling.

IC ₅₀ (µg/mL)	D614G	BA.4.6
COV2-2130 (cilgavimab)	0.095	>10
COV2-2196 (tixagevimab)	0.081	>10
Evusheld	0.066	>10
LY-CoV1404 (bebtelovimab)	0.019	0.009

>10	0.01-0.1	0.001-0.01
-----	----------	------------

Figure S5. Neutralization IC₅₀ titers for authentic D614G and BA.4.6 by clinical mAbs. Background colors indicate neutralization levels.

Supplementary Methods

Patients and vaccinees

Sera from individuals who were vaccinated with three doses of the mRNA-1273 or BNT162b2 vaccine were collected at Columbia University Irving Medical Center (referred to as “boosted” in the text). Sera from individuals who received mRNA vaccinations and were subsequently infected by Omicron subvariant BA.1 or BA.2 were collected at Columbia University Irving Medical Center from December 2021 to May 2022 (referred to as “BA.1 or BA.2 breakthrough” in the text). All samples were examined by anti-nucleoprotein (NP) ELISA to confirm status of prior SARS-CoV-2 infection, and the sequencing was conducted to determine the viral genotype. All subjects provided written informed consent, and all serum collections were performed under protocols reviewed and approved by the Institutional Review Board of Columbia University. Clinical information on different study cohorts is provided in Table S1.

Cell lines

HEK293T cells (CRL-3216) and Vero-E6 cells (CRL-1586) were obtained from the ATCC and were maintained in Dulbecco modified Eagle medium (DMEM) with 10% fetal bovine serum (FBS) and 1% penicillin-streptomycin in an atmosphere of 5% CO₂ at 37°C. Expi293 cells were obtained from Thermo Fisher Scientific (A14527) and were maintained in Expi293TM Expression Medium supplemented with 0.5% penicillin-streptomycin (Thermo Fisher Scientific, Cambridge, MA) at 37°C, 8% CO₂, and 125 rpm.

Monoclonal antibodies

Antibodies (C1520¹, C1717¹, S3H3², amubarvimab³, CAB-A17⁴, Omi-3⁵, Omi-18⁵, BD-515⁶, COVOX-222⁷, XGv347⁸, ZCB11⁹, tixagevimab¹⁰, XGv282⁸, bebtelovimab¹¹, sotrovimab¹², cilgavimab¹⁰, BD55-5840¹³, XGv289⁸, BD55-3152¹³, BD-804¹⁴, romlusevimab³, 2-7¹⁵, 10-40¹⁶) were expressed in-house as previously described¹⁵. Genes of the heavy chain variable (VH) and light chain variable (VL) for each antibody were synthesized (GenScript), cloned into an expression vector (pCMV3 or gWiz), transfected into Expi293 cells using polyethylenimine (PEI), and purified from the supernatants with affinity purification using rProtein A Sepharose (GE) on the fourth day after transfection. Cilgavimab and tixagevimab were obtained from Regeneron Pharmaceuticals.

Construction of SARS-CoV-2 spike plasmids

Plasmids containing spikes of D614G, BA.2, and BA.4/5 were previously constructed¹⁷⁻¹⁹. Expression constructs of the BA.4.6 spike, along with the individual mutations found in BA.4.6, were produced with the QuikChange II XL site-directed mutagenesis kit according to the manufacturer’s instructions (Agilent). To express stabilized soluble spike trimer proteins, 2P substitutions (K986P and V987P in WA1) and a “GSAS” substitution at the furin cleavage site (682-685aa in WA1) were introduced into the spike expression constructs as previously described²⁰. The ectodomain (1-1208aa in WA1) of the spike was then fused with a C-terminal 8x His-tag and cloned into the pAH vector. All constructs were confirmed by Sanger sequencing prior to experiments.

Expression and purification of SARS-CoV-2 stabilized spike trimers and human ACE2

pAH-spike or pcDNA3-sACE2-WT (732)-IgG1 (Addgene plasmid #154104) plasmid was transfected into Expi293 cells using PEI as the transfection reagents, and the supernatants were harvested five days after. To purify the spike proteins, Tris-HCl (pH=8.0) buffer was added at a final concentration of 20mM, and then the solution flowed through the Excel resin (Cytiva) according to the manufacturer’s instructions. For purification of the human ACE2, Protein A Sepharose (Cytiva) was used following the manufacturer’s instructions. All proteins were confirmed by SDS-PAGE, with a purity of approximately 95% before experimental use.

Surface plasmon resonance (SPR)

SPR experiments were performed with a Biacore T200 system equipped with CM5 chips (Cytiva) at ambient temperature (25 °C). The anti-His antibodies were immobilized on the CM5 chip by the His Capture Kit (Cytiva) to reach around 10000 RU. The spike protein was captured on the chip through the C-terminal His-tag, and human ACE2-Fc proteins then flowed through the chip surface at a gradient concentration in HBS-EP+ buffer (Cytiva). The single cycle binding kinetics was analyzed by the Evaluation Software using the 1:1 binding model.

Pseudovirus production

Pseudotyped SARS-CoV-2 were generated in the background of vesicular stomatitis virus (VSV), whose native VSV glycoprotein was replaced with those of SARS-CoV-2 variants as previously described¹⁵. HEK293T cells were transfected with plasmids containing the appropriate spike using 1 mg mL⁻¹ of PEI. The transfected HEK293T cells were cultured under 5% CO₂ at 37 °C for 24 hours, and then they were infected with VSV-G pseudotyped ΔG-luciferase (G*ΔG-luciferase, Kerafast). Two hours after, the infected HEK293T cells were washed three times before being cultured in fresh medium for another 24 hours. The supernatants were then collected, centrifuged to remove precipitates, and aliquoted for storage at -80 °C until the next use.

Pseudovirus neutralization assay

All pseudoviruses were titrated to equilibrate the viral input before each round of neutralization assay. Heat-inactivated sera or antibodies were serially diluted at five-fold in media in triplicate in 96-well plates, starting at 1:100 dilution for sera and 10 μg mL⁻¹ for antibodies. Pseudoviruses were added and the virus-sample mixture was incubated at 37 °C for 1 hour. Control wells that only contained the virus were included on all plates. Vero-E6 cells were then added at a density of 3 × 10⁴ cells per well and the plates were incubated at 37 °C for 10 hours. Cells were lysed and luciferase activity was measured using the Luciferase Assay System (Promega) and SoftMax Pro v.7.0.2 (Molecular Devices) according to instructions from the two manufacturers. ID₅₀ and IC₅₀ values were obtained by fitting a nonlinear five-parameter dose-response curve to the data in GraphPad Prism v.9.2.

Authentic neutralization assay

The nasal swab samples collected in the Columbia University Biobank program²¹ were screened for the mutation R346T in the nsp5 gene using the SNP assay. One viral isolate with R346T genotype was propagated and titrated for the infectivity by the limiting-dilution infectivity assay. The BA.4.6 lineage of this virus was confirmed by the whole viral genome sequencing (GenBank: OP613431; GISAID: EPI_ISL_15327728). The virus neutralization assay was performed in 96-well plate format. Vero-E6 cells were plated at 1.5 × 10⁴ cells/well in DMEM supplemented with 10% FCS and 1x Penicillin/Streptomycin (ThermoFisher). Next day, BA.4.6 virus or D614G control virus (1,500 TCID₅₀) was mixed with the 5-fold dilution series of antibodies, COV2-2130, COV2-2196, Evusheld (AZD7442, AstraZeneca), LY-CoV1404. After 1 hour of incubation at 37 °C, the virus-antibody mixture was inoculated onto the 96 well plates in quadruplicate and cultured at 37 °C with 5% CO₂. On day 3, the CPE was scored (from 0 to 4+) under the inverted microscopy and the IC₅₀ was estimated using GraphPad Prism v.9.2.

Antibody footprint analysis and structural modeling of RBD mutations

The interface residues are generated by using the script from PyMOLwiki. The boundaries of all epitope residues are defined as the antibody footprint and then optimized in Adobe Photoshop. The interaction residues are obtained by CCP4. PyMOL v.2.3.2 was used to perform mutagenesis, to identify hydrogen bonds as well as salt bridge between RBD and antibodies, and to generate structural plots (Schrödinger, LLC).

Quantification and statistical analysis

Serum neutralization ID₅₀ values and antibody neutralization IC₅₀ values were obtained from a five-parameter dose-response curve in GraphPad Prism v.9.2. Statistical significance was evaluated by two-tailed Wilcoxon matched-pairs signed-rank tests using GraphPad Prism v.9.2. Levels of significance are denoted as follows: ns, not significant; *, $P < 0.05$; **, $P < 0.01$; and ***, $P < 0.001$.

Acknowledgements

This study was supported by the NIH SARS-CoV-2 Assessment of Viral Evolution (SAVE) Program. We are grateful to Medini Annavaiahala at Anne-Catrin Uhlemann's lab for sequencing the BA.4.6 isolate by NGS and Boguslaw Wojczyk at Eldad Hod's lab for providing us with the samples from COVID-19 patients.

Author Contributions

Q.W.: data curation, formal analysis, visualization, methodology, validation, project administration, writing-original draft. Z.L.: data curation, formal analysis. J.H. and A.Y.Y.: data curation, methodology. Y.G. and Z.S.: formal analysis. H.M.: resources, data curation. M.L., M.W., J.Y., J.G.S., J.Y.C., F.H., M.T.Y., and M.E.S.: resources. L.L.: conceptualization, supervision, data curation, formal analysis, validation, visualization, methodology, writing-original draft. D.D.H.: conceptualization, supervision, funding acquisition, and writing-review & editing. Q.W. and Z.L. contributed equally.

Declaration of Interests

J.Y., L.L., and D.D.H. are inventors on patent applications (WO2021236998) or provisional patent applications (63/271,627) filed by Columbia University for a number of SARS-CoV-2 neutralizing antibodies described in this manuscript. Both sets of applications are under review. D.D.H. is a co-founder of TaiMed Biologics and RenBio, consultant to WuXi Biologics and Bria Biosciences, and board director for Vicarious Surgical. Other authors declare no competing interests.

Supplementary References

1. Wang Z, Muecksch F, Cho A, et al. Analysis of memory B cells identifies conserved neutralizing epitopes on the N-terminal domain of variant SARS-CoV-2 spike proteins. *Immunity* 2022; **55**(6): 998-1012 e8.
2. Hong Q, Han W, Li J, et al. Molecular basis of receptor binding and antibody neutralization of Omicron. *Nature* 2022; **604**(7906): 546-52.
3. Ju B, Zhang Q, Ge J, et al. Human neutralizing antibodies elicited by SARS-CoV-2 infection. *Nature* 2020; **584**(7819): 115-9.
4. Sheward DJ, Pushparaj P, Das H, et al. Structural basis of Omicron neutralization by affinity-matured public antibodies. *bioRxiv* 2022.
5. Nutalai R, Zhou D, Tuekprakhon A, et al. Potent cross-reactive antibodies following Omicron breakthrough in vaccinees. *Cell* 2022; **185**(12): 2116-31 e18.
6. Cao Y, Yisimayi A, Bai Y, et al. Humoral immune response to circulating SARS-CoV-2 variants elicited by inactivated and RBD-subunit vaccines. *Cell Res* 2021; **31**(7): 732-41.
7. Dejnirattisai W, Zhou D, Supasa P, et al. Antibody evasion by the P.1 strain of SARS-CoV-2. *Cell* 2021; **184**(11): 2939-54 e9.
8. Wang K, Jia Z, Bao L, et al. Memory B cell repertoire from triple vaccinees against diverse SARS-CoV-2 variants. *Nature* 2022; **603**(7903): 919-25.
9. Zhou B, Zhou R, Tang B, et al. A broadly neutralizing antibody protects Syrian hamsters against SARS-CoV-2 Omicron challenge. *Nat Commun* 2022; **13**(1): 3589.
10. Zost SJ, Gilchuk P, Case JB, et al. Potently neutralizing and protective human antibodies against SARS-CoV-2. *Nature* 2020; **584**(7821): 443-9.
11. Westendorf K, Zentelis S, Wang L, et al. LY-CoV1404 (bebtelovimab) potently neutralizes SARS-CoV-2 variants. *Cell Rep* 2022; **39**(7): 110812.
12. Pinto D, Park YJ, Beltramello M, et al. Cross-neutralization of SARS-CoV-2 by a human monoclonal SARS-CoV antibody. *Nature* 2020; **583**(7815): 290-5.
13. Cao Y, Yisimayi A, Jian F, et al. BA.2.12.1, BA.4 and BA.5 escape antibodies elicited by Omicron infection. *Nature* 2022; **608**(7923): 593-602.
14. Du S, Liu P, Zhang Z, et al. Structures of SARS-CoV-2 B.1.351 neutralizing antibodies provide insights into cocktail design against concerning variants. *Cell Res* 2021; **31**(10): 1130-3.
15. Liu L, Wang P, Nair MS, et al. Potent neutralizing antibodies against multiple epitopes on SARS-CoV-2 spike. *Nature* 2020; **584**(7821): 450-6.
16. Liu L, Iketani S, Guo Y, et al. An antibody class with a common CDRH3 motif broadly neutralizes sarbecoviruses. *Sci Transl Med* 2022: eabn6859.
17. Liu L, Iketani S, Guo Y, et al. Striking antibody evasion manifested by the Omicron variant of SARS-CoV-2. *Nature* 2022; **602**(7898): 676-81.
18. Iketani S, Liu L, Guo Y, et al. Antibody evasion properties of SARS-CoV-2 Omicron sublineages. *Nature* 2022; **604**(7906): 553-6.
19. Wang Q, Guo Y, Iketani S, et al. Antibody evasion by SARS-CoV-2 Omicron subvariants BA.2.12.1, BA.4, & BA.5. *Nature* 2022.
20. Wrapp D, Wang N, Corbett KS, et al. Cryo-EM structure of the 2019-nCoV spike in the prefusion conformation. *Science* 2020; **367**(6483): 1260-3.
21. Annavajhala MK, Mohri H, Wang P, et al. Emergence and expansion of SARS-CoV-2 B.1.526 after identification in New York. *Nature* 2021; **597**(7878): 703-8.